Erciyes Üniversitesi
Fen Bilimleri Enstitüsü Dergisi
Cilt 39, Sayı 2, 2023

Erciyes University
Journal of Institute of Science and Technology
Volume 39, Issue 2, 2023

Bio-removal of Remazol black 5 dye by Allium scorodoprasum L. biomass; isotherms, kinetic and thermodynamic studies

Dilek Şenol Arslan[1]

*[1]Abdullah Gul University Engineering Faculty Nanotechnology Engineering, KAYSERİ

(Alınış / Received: 30.04.2023, Kabul / Accepted: 13.07.2023, Online Yayınlanma / Published Online: 31.08.2023)

Keywords
Biosorption
Allium scorodoprasum L.
Isotherm
Kinetic
Thermodynamic

Abstract: The current study aims to use Allium scorodoprasum L. biomass as an biosorbent for the bio-removal of Remazol black 5 (RB5) dye from aqueous solutions. The binding capacity of Allium scorodoprasum L. as a biosorbent for RB5 was investigated by recording the changes in pH, concentration of RB5 dye, biosorbent mass, temperature and contact time. Dubinin-Radushkevich (D-R), Freundlich, and Langmuir isotherm models were used to interpret the experimental data. The maximum RB5 dye biosorption capacity of the biosorbent was found to be 19.8 mg g-1 at 25°C. The biosorption energy indicated that the biosorption process was chemical. Kinetic studies have shown that the biosorption process follows the rate kinetics of PFO and IPD. Thermodynamic studies have shown that RB5 dye biosorption is endothermic and spontaneous. The Allium scorodoprasum L. biomass had a significant biosorption capacity for the anionic RB5 dye.

Remazol black 5 boyasının *Allium scorodoprasum L.* biyokütlesi ile biyolojik olarak uzaklaştırılması; biyosorpsiyon izotermleri, kinetik ve termodinamik çalışmalar

Keywords
Biyosorpsiyon
Allium scorodoprasum L.
İzoterm
Kinetik
Termodinamik

Öz: Bu çalışma, *Allium scorodoprasum L.* biyokütlesini Remazol black 5 (RB5) boyasının sulu çözeltilerden biyo-giderimi için bir biyosorbent olarak kullanmayı amaçlamaktadır. *Allium scorodoprasum L.* biyosorbentinin RB5'e bağlanma kapasitesi, kesikli yürütülen biyosorpsiyon çalışmalarında pH, RB5 boya konsantrasyonu, temas süresi ve sıcaklıktaki değişimler kaydedilerek araştırılmıştır Deneysel verileri açıklamak için Dubinin-Radushkevich (D-R), Freundlich ve Langmuir izoterm modelleri kullanılmıştır. Biyosorbentin maksimum RB5 boya biyosorpsiyon kapasitesi 25 °C'de 19,8 mg g^{-1} olarak bulunmuştur. biyosorpsiyon enerjisi, biyosorpsiyon sürecinin kimyasal olduğunu gösterdi. Kinetik çalışmalar biyosorpsiyon sürecinin PFO ve IPD hız kinetiğini takip ettiğini göstermiştir. Termodinamik çalışmalar RB5 boya biyosorpsiyonunun endotermik spontane olduğunu göstermiştir. Allium scorodoprasum L. biyokütlesi anyonik RB5 boyası için önemli bir biyosorpsiyon kapasitesine sahiptir.

*Corresponding Author, email: dilek.senol@agu.edu.tr

1. Introduction

In recent years, water pollution is an important environmental problem that has received worldwide attention [1]. Industrial wastewater contains a variety of pollutants that are difficult to remove, such as dyes, heavy metals, organics, cyanide, and others [2-5].
The dyes are the main organic pollutants released with industrial textile wastewater because they are highly visible and undesirable in water, even in low quantities [6, 7]. More importantly, most organic dyes are toxic, non-biodegradable, and even teratogenic, carcinogenic and mutagenic, posing serious threats to human health and

marine organisms [8, 9]. In addition, many dye products contain well-known carcinogens such as benzidine or they can produce some other aromatic compounds in the environment via their microbial degradation [10]. Therefore, it is an imperative to treat waste waters in order to eliminate these harmful molecules.
Accordingly, there are many alternative methods are available for address these problems such as; membrane separation, chemical oxidation, adsorption, biosorption, coagulation and precipitation to treat dye-containing wastewaters[11].
Adsorption is the most popular of these methods owing to its low cost, adaptability and simple design, resistance to toxic-substances, and great effectiveness [12, 13]. For the purpose of dye removal from wastewater, natural minerals such as clay [14], vermiculite [15], sepiolite [16], and dolomite [17], as well as natural polymers like chitosan [18] and lignin [19], have become increasingly employed in recent years [20-22].

For the purpose of dye removal from wastewater, natural minerals and polymers as adsorbents including clay [14], vermiculite [15], sepiolite [16], and dolomite [17], as well as natural minerals like chitosan [18] and lignin [19], have become increasingly employed in recent years [20-22].

Adsorption of organic and inorganic materials on the surfaces of either living or dead biomass on their derivatives is referred to as biosorption. Allium is the most popular and distinctive genus in the Alliaceae family, with 750 species categorized into 15 subgenera and 72 sections. *Allium scorodoprasum L*. is a plant that grows 25–90 cm tall and has 1-2 cm-diameter bulbs [23].
Previous studies have shown that Alliaceae family exhibits strong adsorption properties towards heavy metals [24]. It has also shown potential for the removal of organic pollutants, such as dyes and phenols [25, 26].

This study is the first report describing the removal of RB5 dye using the Allium scorodoprasum L. biomass. The objective of this research was to developed an effective biosorbent for removing hazardous industrial dye from wastewater. Allium scorodoprasum L. biomass is a natural, readily available and at the same time low cost biosorbent for the biosorption of colored pollutants. In this study, the biosorbent properties of Allium scorodoprasum L. biomass were investigated for the effective removal of RB5 dye from aqueous solution. The effect of solution pH, biosorbent amount, initial RB5 dye concentration, contact time and temperature on RB5 dye biosorption were investigated using the batch method. The experimental data obtained showed that Allium scorodoprasum L. biomass can be used as an alternative biosorbent for the treatment of wastewater containing RB5 dye.

2. Material and Method
2.1. Material

Allium scorodoprasum L. was collected during July 2022 on Zara, Sivas, Türkiye. RB5 ($C_{26}H_{21}N_5Na_4O_{19}S_6$) was used as a pollutant, which purchased from Sigma-Aldrich (USA) (Fig. 1). Deionized (DI) water was used for all experiments.

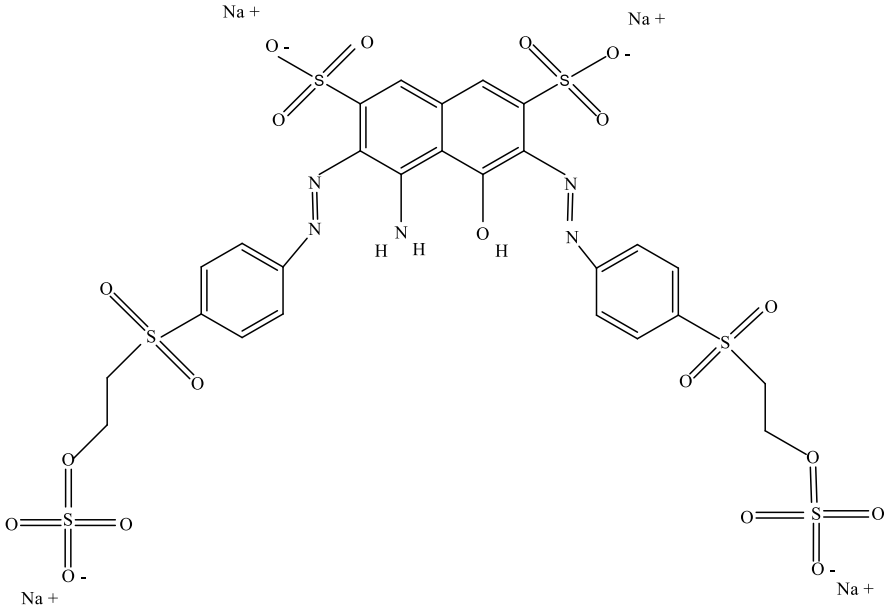

Figure 1. Chemical structure of RB5.

2.1.1. Preparation of *Allium Scorodoprasum L.* Biomass

Allium Scorodoprasum L. samples were cut into small pieces and washed with DI, then dried using traditional sun-drying method. A schematic illustration of *Allium Scorodoprasum L* sample preparation in Fig.2.

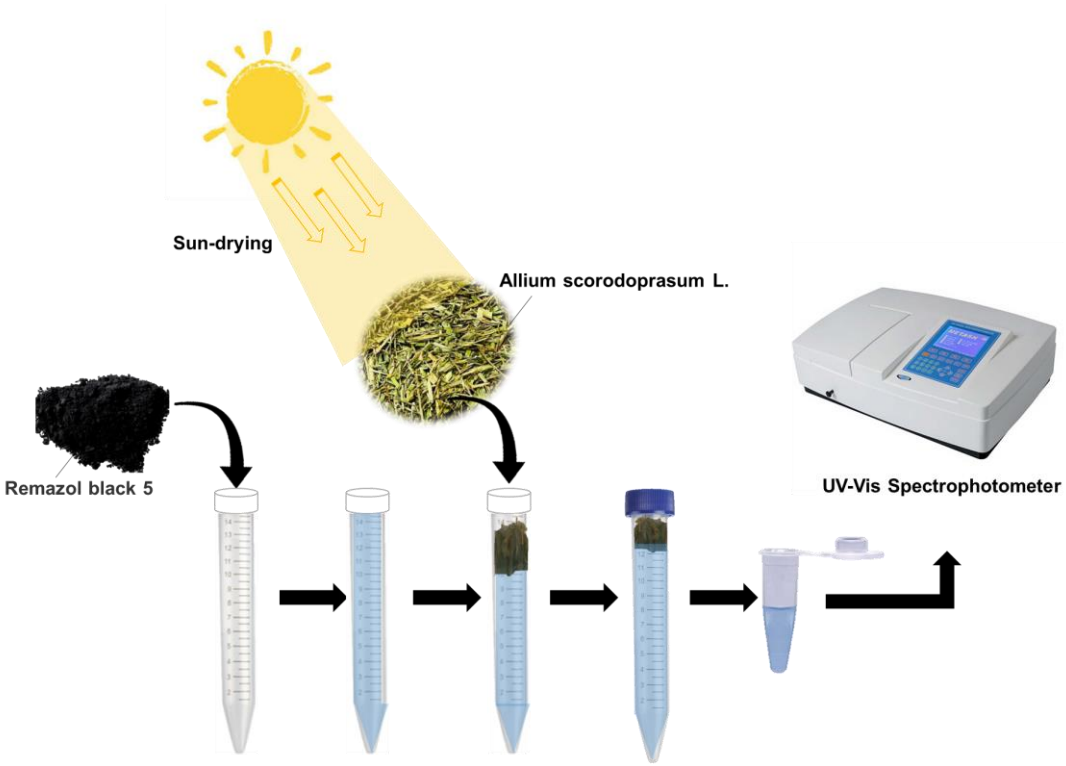

Figure 2. A schematic illustration of *Allium Scorodoprasum L* sample preparation.

2.2. Method

The structure and morphology of *Allium scorodoprasum L* was examined using a scanning electron microscope (Zeiss Gemini) with a 10 kV applied voltage. FT-IR spectra were used to identify the functional properties of g *Allium scorodoprasum L* using an FT-IR spectrometer (Thermo Nicolet Avatar 370). The concentration of Remazol Black 5 was measured with a UV–Visible spectroscopy at a wavelength of 598 nm.

2.2.1. Batch biosorption experiments

A stock RB5 dye solution, 1000 mg L^{-1}, was prepared with DI water. The biosorption of RB5 dye onto *Allium scorodoprasum L* material was performed in 10 mL aqueous solutions, containing 100 mg *Allium scorodoprasum L* material and 200 mg L^{-1} RB5 dye. The experimental conditions pHs (from 2 to 12), and temperature (5 °C, 25 °C, and 40 °C) were fixed. After 24 hours, the supernatant was filtered and the equilibrium RB5 dye concentration was determined at λ=598 nm [27]. Biosorption%, Q (mol kg^{-1}) and desorption % were calculated with Eq. 1, Eq. 2. and Eq. 3

$$Biosorption\% = \left[\frac{C_i - C_f}{C_i}\right] x100 \quad (1)$$

$$Q = \left[\frac{C_i - C_f}{m}\right] xV \quad (2)$$

$$Desorption\% = \frac{Q_{des}}{Q_{ads}} x100 \quad (3)$$

Where, C_i is the initial concentration (mg L^{-1}), C_f is equilibrium concentration (mg L^{-1}), m states to the biosorbent mass (g), V is the solution volume (L), Q_{des}; desorbed amount of RB5 (mg kg^{-1}) and Q_{ads}; biosorbed amount of RB5 (mg kg^{-1}).

3. Results

3.1. FT-IR analysis

Understanding the mechanism of *Allium scorodoprasum L.* surface binding *L* to the RB5 dyes, the functional groups present on the native and after-adsorption plant biosorbent were characterized using an FTIR spectrophotometer. The FTIR spectra of unloaded and RB5 loaded *Allium scorodoprasum L.* biomass shown in Fig.3.

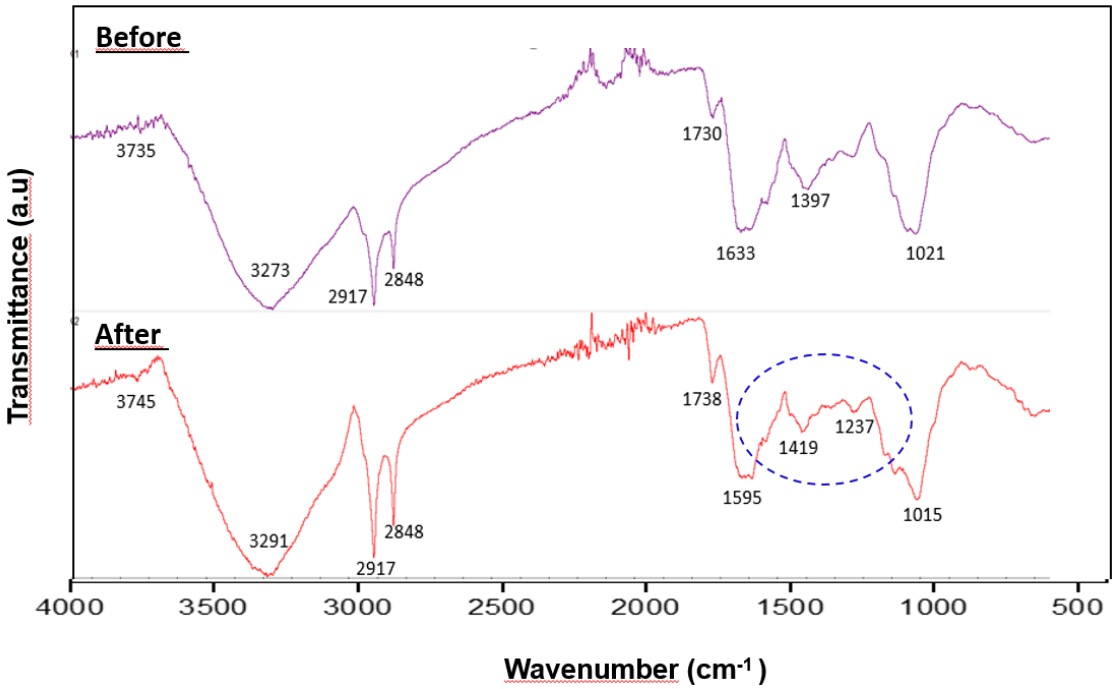

Figure 3. FT-IR spectrum of unloaded and RB5 loaded *Allium scorodoprasum L.* biomass.

Table 1. Assignment of bands to the functional group on the surface of *Allium scorodoprasum L.* as observed from FTIR spectroscopy.

Wave numbers (cm^{-1})		
Unloaded *Allium scorodoprasum L.*	**RB5 Loaded** *Allium scorodoprasum L.*	**Assignment**
3745	3735	O-H stretching/N-H stretching
3273	3291	O-H stretching
2917	2917	CH_2 asymmetric stretching
2848	2848	C-H stretching
1730	1738	C=O stretching vibration.
1633	1595	vibration of H_2O molecules.
1397	1430	vibrations of -CH_2
---	1237	PO_2^- asymmetric and symmetric stretching vibrations
1021	1015	stretching vibrations of -C-O-C.

After RB5 biosorption, -OH and –NH, C=O, C=N, C=C S-O and S-O stretching vibration peaks were shifted. The reason of these shifts are attributed to the interaction between functional groups on the surface of *Allium scorodoprasum L* and RB5. The azo dyes showed a strong band at ~1730 cm^{-1} due to ν(C=O)[28].

3.2. SEM analysis

The plant's morphology was determined using scanning electron microscopy, which was also utilized to take photos of the microstructures. This technique can be utilized to comprehend the morphology and behavior of the plant both before and after the dye has been biosorbed.

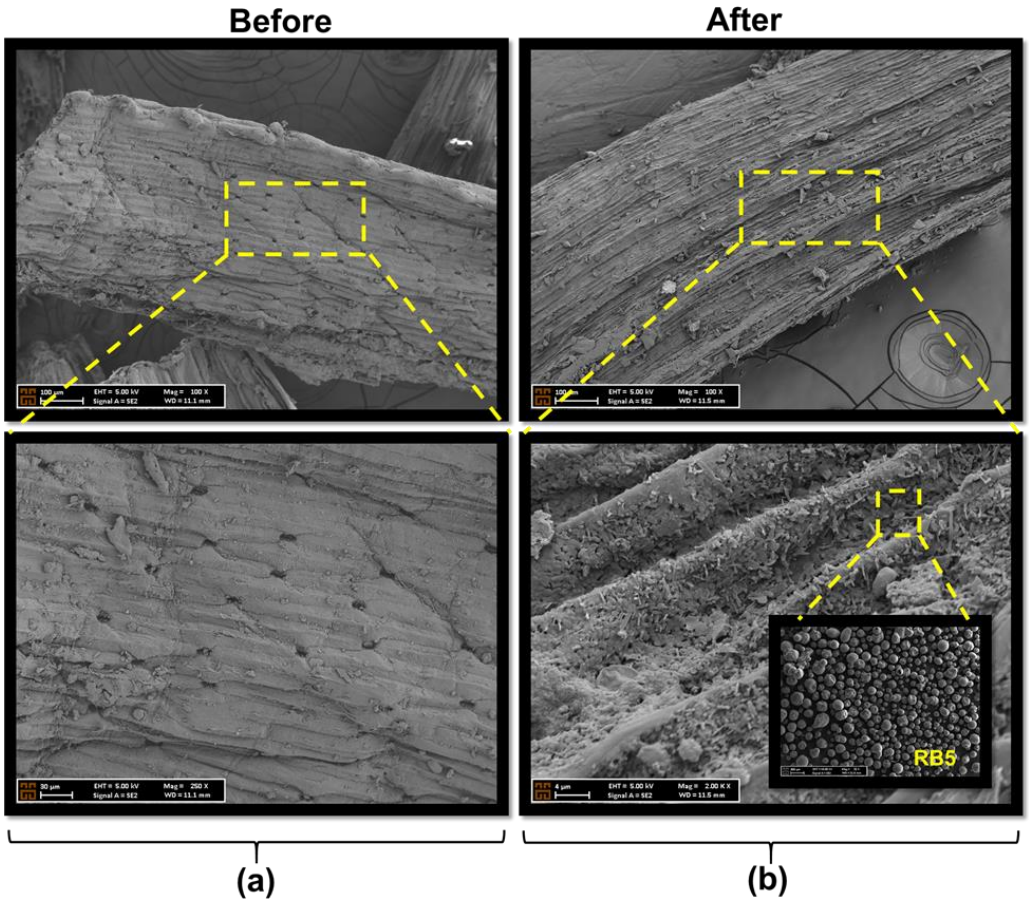

Figure 4. SEM images of RB5 biosorption before (a) and after (b).

As seen in Fig. 4, RB5 dye aggregates filled the gaps and clustered within the layers of the bio-composite surface, as a result of the biosorption processes. SEM analysis was used to visualize the presence of pores and the inner surface before adsorption; the image taken after biosorption of RB5 dye showed that the porous structure was filled by biosorption and RB5 was deposited on the Allium scorodoprasum L. surface. SEM pictures demonstrate that the presence of a large amount of aggregates on the biosorbent surface indicates that the biosorbent is an excellent material for dye biosorption.

3.3. Effect of inital pH and PZC for *Allium scorodoprasum L.* biomass

The biosorption of the RB5 dye onto *Allium scorodoprasum L.* biosorbent in solutions with different pH values is shown in Figure 5. Biosorption results has indicated that a sharp decrease between pH 2.0 and 4.0. After this point, it gradually decreased (pH: 4.0-8.0). The point of zero charge (pHpzc) of *Allium scorodoprasum L.* biosorbent was found 5.72. The surface (pH<pHpzc) of the *Allium scorodoprasum L* biosorbent was positive at acidic pHs. In this case, H^+ ions and anionic RB5 dye molecules competed for binding to active sites on the surface of the *Allium scorodoprasum L.* biosorbent. The *Allium scorodoprasum L.* biosorbent, which has a positively surface charge, electrostatically attracted the anionic RB5 dye molecules. Therefore, the biosorption efficiency was high at acidic pHs. At alkaline pHs above the pHpzc, the surface of the *Allium scorodoprasum L.* biosorbent was negative. The *Allium scorodoprasum L.* biosorbent, which had a negatively surface charge, so electrostatically repulsed the anionic RB5 dye molecules. As a result, the biosorption efficiency decreased.

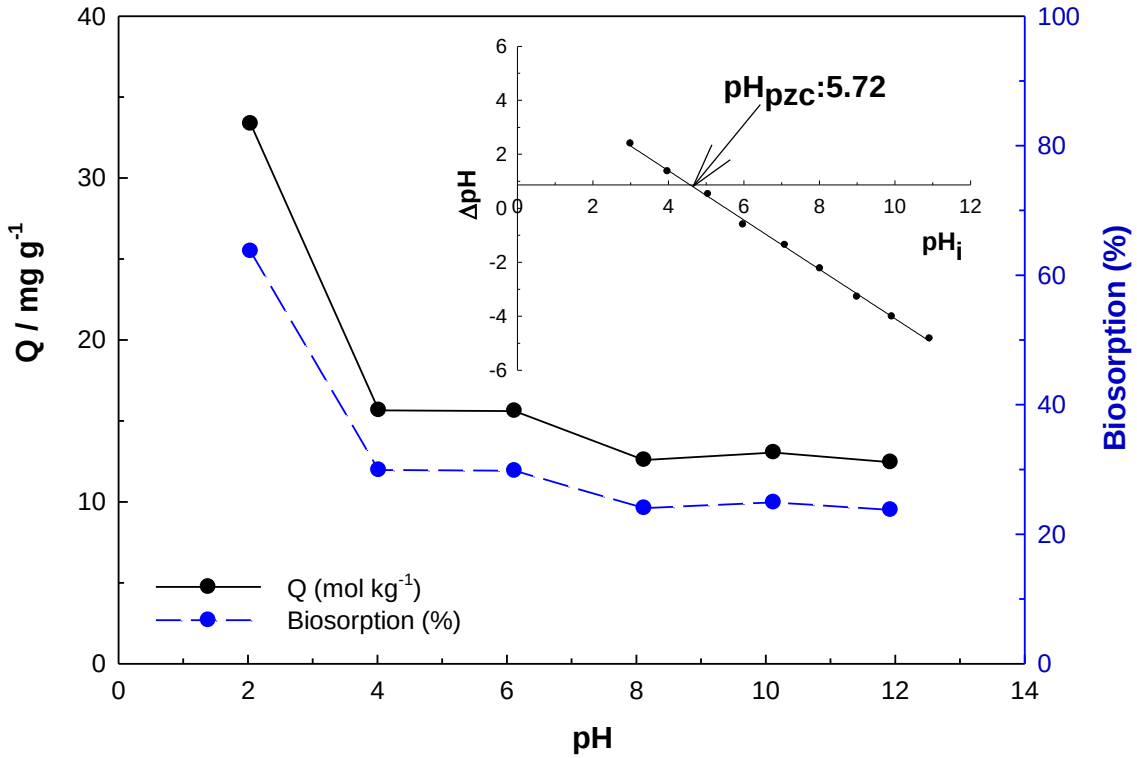

Figure 5. Effect of pH on RB5 biosorption onto *Allium scorodoprasum L.* and pzc for *Allium scorodoprasum L.*

3.4 Effect of biosorbent mass

Biosorption behavior was examined between 1 g L^{-1} and 10 g L^{-1} (Figure 6). RB5 dye biosorption increased with the increase in the amount of *Allium scorodoprasum L.* biosorbent. Up to a certain point, the action centers on the surface of the *Allium scorodoprasum L.* biosorbent increased as the amount of biosorbent increased. Thus, RB5 dye molecules more easily penetrated the action centers on the *Allium scorodoprasum L.* biosorbent surface. The maximum amount of biosorption was found to be about 57% at 10 g L^{-1} of the *Allium scorodoprasum L.* biosorbent. Thus, the increase in RB5 dye biosorption efficiency was a function of the increase in active binding sites.

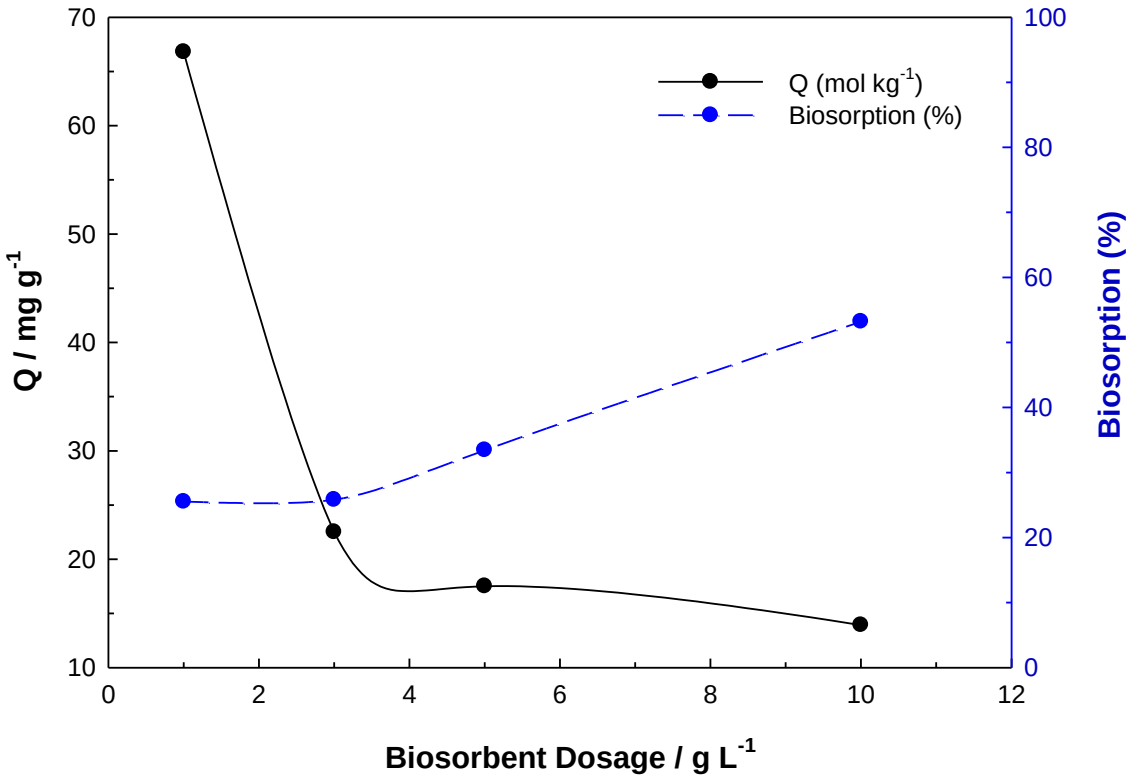

Figure 6. Effect of biosorbent mass on RB5 biosorption onto *Allium scorodoprasum L.*

3.4. Modeling of Biosorption Process

Biosorption isotherms provided very useful data to understand the biosorption mechanism. Isotherm models were used to describe the behaviour of dye-biosorbent pairs. The Dubinin-Radushkevich (D-R), Langmuir, and Freundlich models were employed in this study to explore the interaction between RB5 dye molecules and the biosorbent surface of *Allium scorodoprasum L*. The parameters indicated in Table 2 have been calculated using the equations below for the biosorption isotherm models (Eq. 4, 5, 6, 7, and 8).

$$Q = \frac{X_L K_L C_e}{1+K_L C_e} \quad (4)$$

$$Q = K_F C_e^{\beta} \quad (5)$$

$$Q = X_{DR} e^{-K_{DR}\varepsilon^2} \quad (6)$$

$$\varepsilon = RTln(1+\frac{1}{C_e}) \quad (7)$$

$$E_{DR} = (2K_{DR})^{-0.5} \quad (8)$$

Because of the emptiness of active centres on the *Allium scorodoprasum L.* biosorbent surface, RB5 dye biosorption effectiveness was shown to be high at low concentrations. At high concentrations, however, due to the filling of all active centres on the *Allium scorodoprasum L.* biosorbent surface, it decreased and eventually reached to an equilibrium. When the R^2 values from the Langmuir and Freundlich isotherm models were examined, the biosorption process fit the Langmuir isotherm model better. The Langmuir model predicts that the adsorbent surface's active sites are uniformly distributed [29].

The capacity of monolayer biosorption was discovered to be 19.8. mg g^{-1}. In Langmuir, it was 0.00525 L mg^{-1}. The Freundlich isotherm model is based on multilayer biosorption on heterogeneous surfaces and provides information on heterogeneity of the biosorbent surface. [30]. The Freundlich biosorption capacity was found to be X_F, 0.465, and the β surface heterogeneity was 0.563. The D-R model investigates the biosorption process in terms of energy [31]. The biosorption energy of RB5 dye was found to be 9.83. kJ mol^{-1}. Thus, this finding indicated that a chemical biosorption took place.

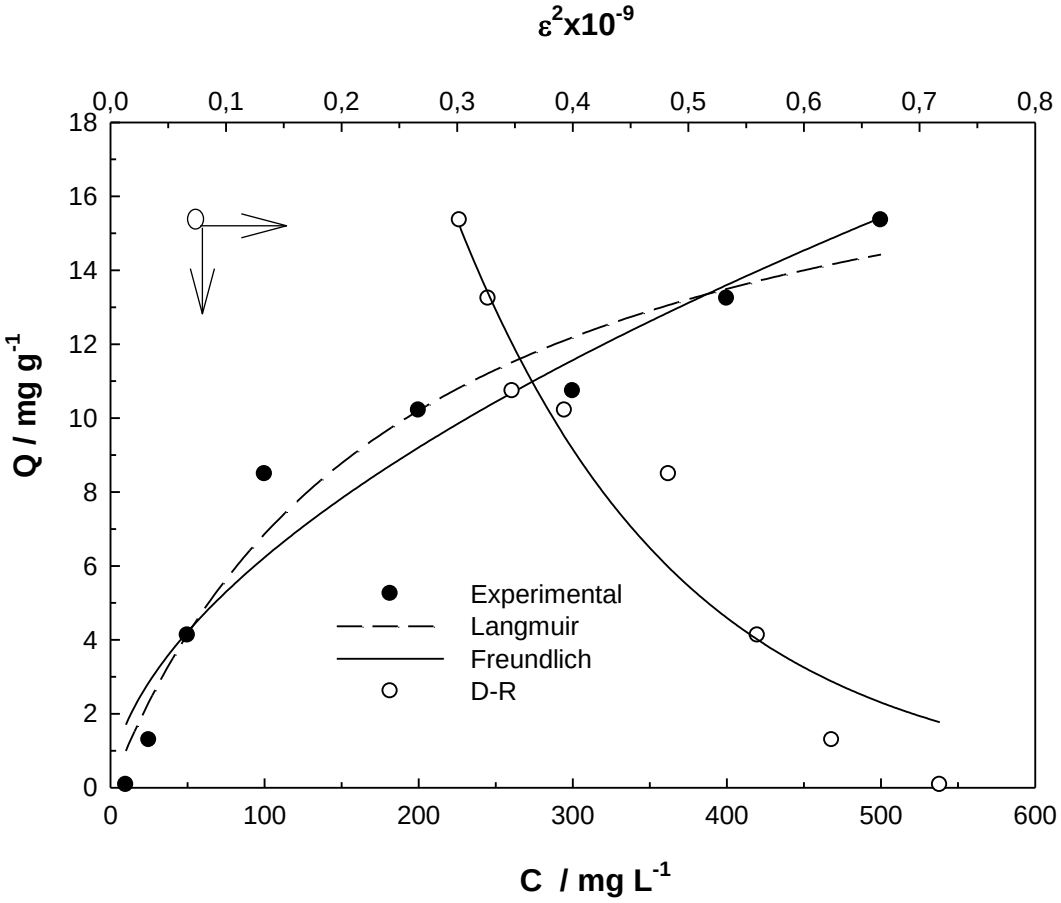

Figure 7. Langmuir, Freundlich and D-R models.

Table 2. Langmuir, Freundlich and D-R isotherm models parameters

Isotherm	Value	R^2
Langmuir		
X_L (mg g^{-1})	19.8	0.965
K_L (L mg^{-1})	0.00525	
Freundlich		
X_F	0.465	0.945
β	0.563	
D-R		
X_{DR} (mg g^{-1})	72.5	0.936
$-K_{DR}x10^9$/mol^2KJ^{-2}	5.17	
E_{DR}/kJ mol^{-1}	9.83	

3.5. Effect of contact time on biosorption

The kinetic study is crucial in finding the optimum interaction time of the *Allium scorodoprasum L.* biosorbent and the RB5 dye. To explain the RB5 dye biosorption kinetics of *Allium scorodoprasum L.* biosorbent, pseudo first order (PFO) [32] and pseudo second order kinetic models (PSO), [33], and intraparticle diffusion (IPD) [34] were applied and and the kinetic parameters were derived using the following equations (Eq.9, 10, 11, 12, and 13)

$$Q_t = Q_e\left[1 - e^{-k_1 t}\right] \quad (9)$$

$$H_1 = k_1 Q_e \quad (10)$$

$$Q_t = \frac{t}{\left[\frac{1}{k_2 Q_e^2}\right] + \left[\frac{t}{Q_e}\right]} \quad (11)$$

$$H_2 = k_2 Q_e^2 \quad (12)$$

$$Q_t = k_i t^{0.5} \quad (13)$$

The RB5 dye biosorption reached equilibrium in 240 minutes (4 hours) (Figure 8). When the correlation coefficients (R^2) of the PFO and PSO models were examined, it was discovered that the PFO kinetic model fit the data better. Furthermore, the similarity between the theoretically estimated Qt and practical Qe values revealed in compliance with the PFO model. The presence of two line components in the IPD model graph rather than a single line passing through the origin indicated that biosorption encompassed various diffusion stages that occurred both on and inside the surface.

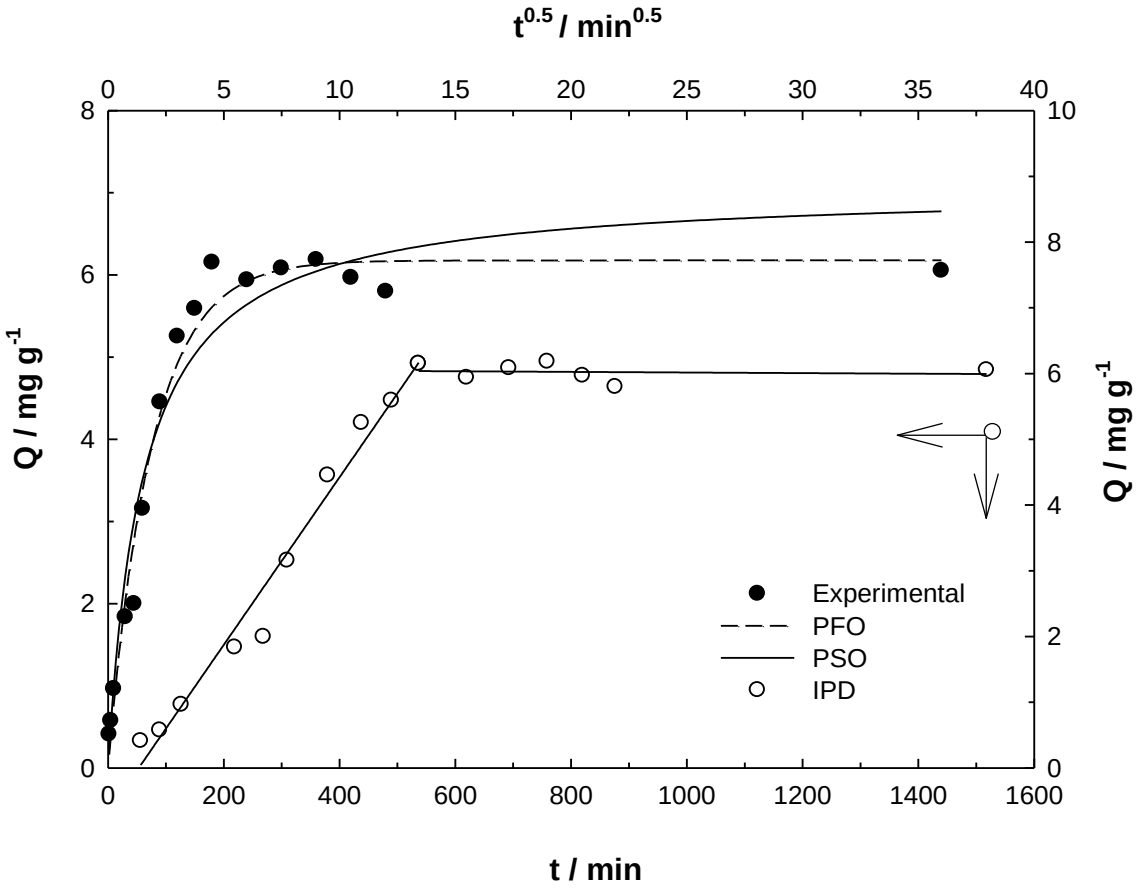

Figure 8. PFO, PSO and IPD models.

Table 3. PFO, PSO and IPD kinetic models parameters

Kinetic model	Value	R^2
Pseudo first order		
Q_t/mg g^{-1}	6.05	0.980
Q_e/mg g^{-1}	6.18	
k_1 x10^3/min^{-1}	13.2	
Hx10^3/mg g^{-1} min^{-1}	81.6	
Pseudo second order		
Q_t/mg g^{-1}	6.05	0.950
Q_e/mg g^{-1}	7.06	
k_2 x10^3/mg^{-1} g min^{-1}	2.35	
Hx10^3/mg $g^{-1}$$min^{-1}$	117	
Intra particle diffusion		
k_i x10^3/mg g^{-1} $min^{-0.5}$	676	0.977

3.6. Effect of temperature

In the process of the biosorption procedure, the thermodynamic parameters for RB5 dye biosorption to *Allium scorodoprasum L* biosorbent, namely free Gibbs energy (ΔG^0), enthalpy (ΔH^0), and entropy (ΔS^0) of biosorption can be evaluated using the equations given (Eq. 14,15 and 16).

$$K_D = \frac{Q}{C_e} \quad (14)$$

$$\Delta G^0 = -RTlnK_D \quad (15)$$

$$lnK_D = \frac{\Delta S^0}{R} - \frac{\Delta H^0}{RT} \quad (16)$$

The ΔH^0 value was determined to be 7.55 kJ mol^{-1}. The positive ΔH^0 value was proved that the biosorption process of RB5 dye molecules was endothermic. The value of entropy was found to be 58.2 J mol^{-1} K^{-1}. In a solid-liquid system, the biosorption process led to the production of hydrated molecules. The positive ΔS^0 value showed a rise in a random interaction at the solid-liquid interface during the biosorption process. The ΔG^0 values were -8.6 kJ mol^{-1}, -9.2 kJ mol^{-1}, -9.8 kJ mol^{-1}, -10.7 kJ mol^{-1} and -11.3 kJ mol^{-1} at 5°C, 15°C, 25°C, 40°C, and 50°C, respectively. The decline in ΔG^0 value as temperature increased demonstrated that biosorption of RB5 dye molecules into *Allium scorodoprasum L.* biosorbent was possible, effective, and spontaneous at high temperature. According to the thermodynamic data, the RB5 biosorption process to the *Allium scorodoprasum L* biosorbent was spontaneous, endothermic, and increasing with entropy.

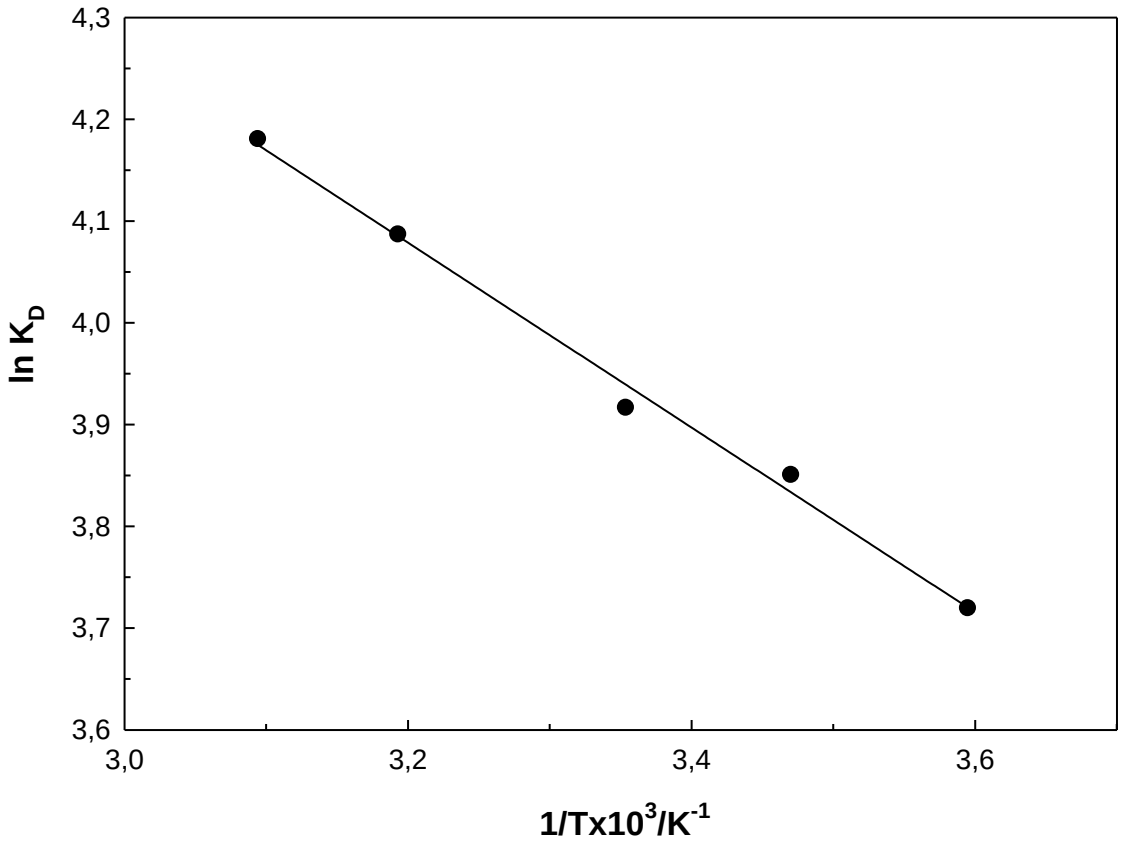

Figure 9. The effect of temperature on the biosorption

4. Discussion and Conclusion

In this study, the potential use of *Allium scorodoprasum L*. biomass as adsorbent for the bioremoval of RB5 dye from aqueous solutions. The results above discussed indicated that;

- The *Allium scorodoprasum L*. biosorbent and optimum reaction conditions for RB5 dye removal were determined for maximum biosorption as follows: natural dye pH, biosorbent mass: 100 mg, contact time 24 h, and temperature 25°C.
- The maximum biosorption capacity of the biosorbent for IC was found to be 19.8 mg g^{-1} at 25 °C (R^2 values, Langmuir isotherm model). As a result, the Langmuir model best fit the results.
- The E_{DR}: 9.83 kJ mol^{-1}, indicated that the RB5 dye biosorption process to the *Allium scorodoprasum L*. biosorbent was chemical.
- The biosorption kinetic process followed the PFO and IPD kinetics.
- The thermodynamic properties indicate that the biosorption process is spontaneous and endothermic.
- The biosorbed RB5 on the surface of the *Allium scorodoprasum L*. biosorbent was also proven by FT-IR spectra and visualized by SEM.
- In light of all these findings, it was concluded that *Allium scorodoprasum L.* biomass can be used as an effective and alternative biosorbent for the removal of RB5 impurities from industrial wastewater.

References

[1] Chaudhry, F.N. and M. Malik, *Factors affecting water pollution: a review.* J. Ecosyst. Ecography, 2017. **7**(1): p. 225-231.

[2] Ajiboye, T.O., O.A. Oyewo, and D.C. Onwudiwe, *Simultaneous removal of organics and heavy metals from industrial wastewater: A review.* Chemosphere, 2021. **262**: p. 128379.

[3] Namasivayam, C., D. Sangeetha, and R. Gunasekaran, *Removal of anions, heavy metals, organics and dyes [from water by adsorption onto a new activated carbon from Jatropha husk, an agro-industrial solid waste.* Process Safety and Environmental Protection, 2007. **85**(2): p. 181-184.

[4] Khan, F.S.A., et al., *A comprehensive review on magnetic carbon nanotubes and carbon nanotube-based buckypaper for removal of heavy metals and dyes.* Journal of Hazardous Materials, 2021. **413**: p. 125375.

[5] Palani, G., et al., *Current trends in the application of nanomaterials for the removal of pollutants from industrial wastewater treatment—a review.* Molecules, 2021. **26**(9): p. 2799.

[6] Saini, R.D., *Textile organic dyes: polluting effects and elimination methods from textile waste water.* Int J Chem Eng Res, 2017. **9**(1): p. 121-136.

[7] Carmen, Z. and S. Daniela, *Textile organic dyes-characteristics, polluting effects and separation/elimination procedures from industrial effluents-a critical overview*. Vol. 3. 2012: IntechOpen Rijeka.

[8] Brillas, E. and C.A. Martínez-Huitle, *Decontamination of wastewaters containing synthetic organic dyes by electrochemical methods. An updated review.* Applied Catalysis B: Environmental, 2015. **166**: p. 603-643.

[9] Goyal, P., C.S. Tiwary, and S.K. Misra, *Ion exchange based approach for rapid and selective Pb (II) removal using iron oxide decorated metal organic framework hybrid.* Journal of Environmental Management, 2021. **277**: p. 111469.

[10] Kariminiaae-Hamedaani, H.-R., A. Sakurai, and M. Sakakibara, *Decolorization of synthetic dyes by a new manganese peroxidase-producing white rot fungus.* Dyes and Pigments, 2007. **72**(2): p. 157-162.

[11] Priyan, V.V., et al., *Ecotoxicological assessment of micropollutant Diclofenac biosorption on magnetic sawdust: Phyto, Microbial and Fish toxicity studies.* Journal of Hazardous Materials, 2021. **403**: p. 123532.

[12] Islam, A., et al., *Step towards the sustainable toxic dyes removal and recycling from aqueous solution-A comprehensive review.* Resources, Conservation and Recycling, 2021. **175**: p. 105849.

[13] Kubra, K.T., M.S. Salman, and M.N. Hasan, *Enhanced toxic dye removal from wastewater using biodegradable polymeric natural adsorbent.* Journal of Molecular Liquids, 2021. **328**: p. 115468.

[14] Paredes-Quevedo, L.C., et al., *Removal of a textile azo-dye (Basic Red 46) in water by efficient adsorption on [a natural clay.* Water, Air, & Soil Pollution, 2021. **232**: p. 1-19.

[15] Shen, T., et al., *Single and simultaneous adsorption of basic dyes by novel organo-vermiculite: A combined experimental and theoretical study.* Colloids and Surfaces A: Physicochemical and Engineering Aspects, 2020. **601**: p. 125059.

[16] Largo, F., et al., *Adsorptive removal of both cationic and anionic dyes by using sepiolite clay mineral as adsorbent: Experimental and molecular dynamic simulation studies.* Journal of Molecular Liquids, 2020. **318**: p. 114247.

[17] Shirazi, E.K., et al., *Removal of textile dyes from single and binary component systems by Persian bentonite and a mixed adsorbent of bentonite/charred dolomite.* Colloids and Surfaces A: Physicochemical and Engineering Aspects, 2020. **598**: p. 124807.

[18] Ngah, W.W., L. Teong, and M.M. Hanafiah, *Adsorption of dyes and heavy metal ions by chitosan composites: A review.* Carbohydrate polymers, 2011. **83**(4): p. 1446-1456.

[19] Lee, S.-L., et al., *Sorption behavior of malachite green onto pristine lignin to evaluate the possibility as a dye adsorbent by lignin.* Applied Biological Chemistry, 2019. **62**: p. 1-10.

[20] Göçenoğlu Sarıkaya, A., *Kinetic and thermodynamic studies of the biosorption of Cr (VI) in aqueous solutions by Agaricus campestris.* Environmental Technology, 2021. **42**(1): p. 72-80.
[21] Dalvi, V., et al., *Removal of pollutants from wastewater via biological methods and shifts in microbial community profile during treatment process.* Wastewater Treatment Reactors, 2021: p. 19-38.
[22] Kumar, A., et al., *Biosorption: The removal of toxic dyes from industrial effluent using phytobiomass-A review.* Plant Arch, 2021. **21**: p. 1320-1325.
[23] Tasci, B. and I. Koca. *Use of Allium scorodoprasum L. subsp. rotundum as food*. in *VII International Symposium on Edible Alliaceae 1143*. 2015.
[24] Sheikh, Z., et al., *Potential application of Allium Cepa seeds as a novel biosorbent for efficient biosorption of heavy metals ions from aqueous solution.* Chemosphere, 2021. **279**: p. 130545.
[25] Đorđevski, N., et al., *Chemical and Biological Investigations of Allium scorodoprasum L. Flower Extracts.* Pharmaceuticals, 2022. **16**(1): p. 21.
[26] Demir, T., et al., *Phenolic profile and investigation of biological activities of Allium scorodoprasum L. subsp. rotundum.* Food Bioscience, 2022. **46**: p. 101548.
[27] Cristóvão, R.O., et al., *Modeling the discoloration of a mixture of reactive textile dyes by commercial laccase.* Bioresource Technology, 2009. **100**(3): p. 1094-1099.
[28] Peplowski, L., et al., *Vibrational spectroscopy studies of methacrylic polymers containing heterocyclic azo dyes.* Vibrational Spectroscopy, 2022. **120**: p. 103377.
[29] Olawale, S.A. and O.O. Oluwasina, *Kinetics Studies for the Adsorption of Aqueous Cu (II) and Pb (II) Ions onto Chicken Feather.* Langmuir, 1918. **2**(W3): p. W2-W1.
[30] Rajabi, M., et al., *Comparison and interpretation of isotherm models for the adsorption of dyes, proteins, antibiotics, pesticides and heavy metal ions on different nanomaterials and non-nano materials—a comprehensive review.* Journal of Nanostructure in Chemistry, 2023. **13**(1): p. 43-65.
[31] Dubinin, M., *Modern state of the theory of gas and vapour adsorption by microporous adsorbents.* Pure and Applied Chemistry, 1965. **10**(4): p. 309-322.
[32] Ho, Y.-S. and G. McKay, *Sorption of dye from aqueous solution by peat.* Chemical engineering journal, 1998. **70**(2): p. 115-124.
[33] Ho, Y.-S. and G. McKay, *Pseudo-second order model for sorption processes.* Process biochemistry, 1999. **34**(5): p. 451-465.
[34] Weber Jr, W.J. and J.C. Morris, *Kinetics of adsorption on carbon from solution.* Journal of the sanitary engineering division, 1963. **89**(2): p. 31-59.